JOURNAL OF GEOPHYSICAL RESEARCH, VOL. 106, NO. D24, PAGES 33,691–33,705, DECEMBER 27, 2001

Program for Arctic Regional Climate Assessment (PARCA): Goals, key findings, and future directions

Robert H. Thomas[1] and PARCA Investigators

Abstract. The NASA Program for Arctic Regional Climate Assessment (PARCA) has the prime objectives of measuring and understanding the mass balance of the Greenland ice sheet. It includes measurement of changes in ice sheet volume using different approaches, analysis of satellite and aircraft data to investigate various characteristics of the ice sheet, and in situ measurements aimed at understanding observed changes. The most important result from PARCA is the first accurate assessment of the mass balance of a polar ice sheet. Higher-elevation parts of the ice sheet are in overall balance, with local areas of quite rapid thickening or thinning, most of which could represent the effects of temporal variability in snow accumulation rates. Many coastal regions thinned considerably during the 1990s, with net losses from the ice sheet sufficient to raise global sea level by almost 10% of the total increase. There was coastal warming during this period, and a network of automatic weather stations (AWS) on the ice sheet measured a 2° warming for 1995–1999 compared to the 1950s. Nevertheless, observed ice-thinning rates of up to several meters per year cannot be explained by increased melting, indicating that discharge velocities must also have increased. In addition to the scientific results, major advances have been made in the use of satellite data for ice sheet research, particularly application of synthetic aperture radar (SAR) data to the measurement of ice velocity and identification and monitoring of glacier grounding lines. On the basis of these observations, PARCA focus has shifted to the coastal regions, with emphasis on surface ablation and its sensitivity to summer warming and possible albedo feedback, and on the dynamics of the glaciers that are observed to be changing rapidly.

1. Introduction

Key to any assessment of future sea level change is the mass balance of the Greenland and Antarctic ice sheets: are they increasing or decreasing in volume? Currently, the uncertainty in their mass-balance estimates is approximately equivalent to the observed global sea level rise. The Program for Arctic Regional Climate Assessment (PARCA) is a NASA project with the prime goal of addressing this issue for Greenland. It was formally initiated in 1995 by combining into one coordinated program various investigations associated with efforts, started in 1991, to assess whether airborne laser altimetry could be applied to measure ice sheet thickness changes. The prime result is an order-of-magnitude improvement in our estimates for the mass balance of the entire ice sheet, with quite detailed assessments of the behavior of smaller regions within the ice sheet. Significant progress has also been made in the development of new techniques for glaciological research and in process studies. Taken as a whole, results from PARCA represent a significant advance in our knowledge and understanding of the mass balance of the Greenland ice sheet, and they form a baseline set of measurements for comparison with precise surface elevation data to be acquired by the NASA Geoscience Laser Altimeter System (GLAS) aboard ICESAT, which will be launched in the latter part of 2001. This special section presents the major results from the program to date, with an assessment of our current understanding of the mass balance of the ice sheet, and this introductory paper provides a brief description of the Greenland ice sheet and major differences between it and the Antarctic ice sheet, an outline of the PARCA approach to measuring and understanding the ice sheet mass balance, a summary of key results from the program, and recommendations for future research to address issues revealed by the PARCA results. Place names and locations referred to in what follows can be found in the foldout map provided with the special section.

2. Polar Ice Sheets

The Greenland ice sheet occupies a latitude band extending from 60°N to 80°N and covers an area of 1.7 million square kilometers. With an average thickness of 1600 m, it has a total volume of ~3 million cubic kilometers, equivalent to a sea level rise of about 7 m. It consists of a northern dome and a southern dome, with maximum surface elevations of ~3200 and 2850 m, respectively, linked by a long saddle with elevations around 2500 m. Bedrock beneath much of the ice sheet is close to sea level, but the ice sheet is fringed almost completely by coastal mountains through which the ice sheet is drained by many glaciers.

The ice sheet in Greenland differs significantly from that in Antarctica, which is almost 10 times larger in volume. Antarctica straddles the South Pole and has a dominant influence on its own climate and on the surrounding ocean, with cold conditions even during the summer and around its northern margins. Away from the coast, much of Antarctica is a cold desert, with very low precipitation rates. There is little surface melting, even near the coast, and most of the meltwater soaks into

[1]EG&G, Inc., Wallops Flight Facility, Wallops Island, Virginia.

Copyright 2001 by the American Geophysical Union.

Paper number 2001JD900042.
0148-0227/01/2001JD900042$09.00

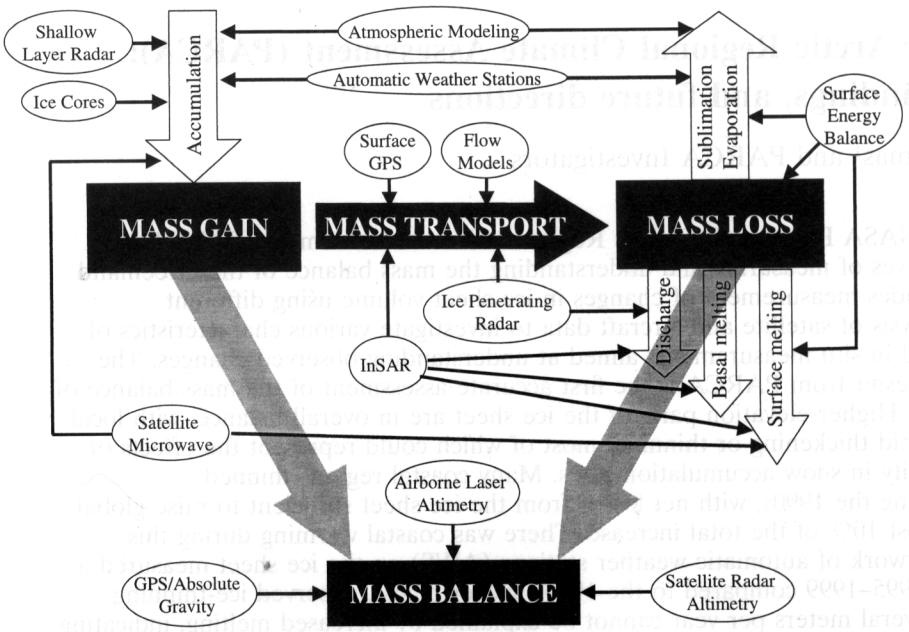

Figure 1. PARCA, showing links between the various activities.

underlying snow and refreezes. Because of the cold conditions, vast floating ice shelves exist around much of the continent. Ice drainage is primarily by glaciers and ice streams, some of which penetrate deep into the heart of the ice sheet, moving at maximum speeds of a few hundred meters per year, apart from a few exceptions. Most glaciers and ice streams flow into ice shelves, which are also fed by snow accumulation on their surfaces. The ice shelves thin toward their seaward ice fronts, partly by ice creep and partly by basal melting, with melting rates generally of a few tens of centimeters per year. Thus ice loss from the Antarctic ice sheet is primarily by melting and iceberg calving from ice shelves.

By contrast, the Greenland climate is strongly affected by its proximity to other landmasses and to the North Atlantic, with the Gulf Stream to the south and regions of North Atlantic deep water production to the east and west. Ice core data from the summit of the Greenland ice sheet indicate that Greenland temperatures and accumulation rates can increase significantly over periods of a few years to decades [*Alley et al.*, 1993]. Other major contrasts with Antarctica include widespread summer melting, higher accumulation rates, very few ice shelves, and faster glaciers. Summer melting occurs over about 50% of the ice sheet surface, depending on summer temperatures, with much of the resulting meltwater flowing into the sea, either along channels cut into the ice surface or by draining to the bed via crevasses. The average accumulation rate (~0.3 m water/year) is more than double that for Antarctica, so although the ice sheet is far smaller, its total annual exchange of water with the ocean is about 30% that for Antarctica. Higher coastal temperatures in Greenland do not favor ice shelves, but there are a few along the north and northeast coasts. Basal melting from these reaches values exceeding 10 m/yr, and they give an indication of the potential effect of warmer ocean temperatures around Antarctica. Most Greenland outlet glaciers are narrower, by an order of magnitude, than their Antarctic counterparts, but some reach speeds that are an order of magnitude larger. Consequently, these glaciers drain very large volumes of ice, with discharge rates strongly determined by fast-glacier dynamics, which are poorly understood.

3. Program for Arctic Regional Climate Assessment (PARCA)

The PARCA inception owed most to the Global Positioning System (GPS) of satellites. By the late 1980s these were sufficiently well established and data analysis techniques sufficiently mature to offer the possibility of providing very precise knowledge of aircraft trajectories via kinematic solutions of GPS data acquired aboard the aircraft [*Krabill and Martin*, 1987]. Until then, the lack of such knowledge had seriously limited measurement of absolute surface topography from aircraft, and the measurement of small changes associated with ice sheet thickening or thinning was out of the question. Consequently, starting in 1991, the NASA Polar Research Program sponsored an exhaustive series of tests in Greenland to assess the accuracy of an existing scanning laser altimeter flown aboard a GPS-equipped aircraft over the ice sheet [*Krabill et al.*, 1995]. Soon afterward, this program was enhanced by development and airborne testing of a coherent ice-depth-sounding radar [*Gogineni et al.*, 1998]. Results were sufficiently promising to warrant an aircraft survey in 1993 and 1994 of both surface elevation and ice thickness over all the major ice drainage basins on the ice sheet, with the intention of repeating these surveys in the future to determine elevation changes.

During this period, other events occurred which helped establish a basis for PARCA: synthetic aperture radar (SAR) data from the ERS-1 satellite were used to compile a mosaic map of Greenland [*Fahnestock et al.*, 1993] and to infer ice velocities by interferometric analysis of time-separated image pairs [*Goldstein et al.*, 1993]; research was ongoing on the interpretation of time series of satellite microwave data in terms of ice-surface characteristics; analysis of the effects of interannual variability of snow accumulation rates indicated that these alone could cause quite large rates of ice-surface

elevation change over periods of several years [*Braithwaite*, 1993; *van der Veen*, 1993]; and ice core analyses were providing more precise annual resolution due to use of continuous flow techniques, identification of multiple seasonally varying parameters, and a strong commitment to high-precision dating [*Anklin et al.*, 1998; *Mosley-Thompson et al.*, this issue]. Consequently, in 1995, PARCA was formally established, comprising the following key elements: (1) direct measurement of ice surface elevation change from time series of satellite radar- and aircraft laser-altimeter data; (2) localized measurements of long-term ice thickness change from measurements of the vertical motion of markers buried in the ice; (3) indirect "mass-budget" estimates of long-term changes in ice sheet volume by comparing total snow accumulation with total ice discharge; (4) historical ice thickness change inferred from precise GPS and gravity measurements of crustal motion at coastal sites on each side of the ice sheet; (5) ice core acquisition and analysis to improve estimates of total snow accumulation and its long-term trends and to assess the impacts on surface-elevation change of interannual variability in snow accumulation rates; (6) estimation of snow accumulation rates at high temporal resolution, by model assimilation of analysis fields provided by global weather models, and validation by analysis of high-resolution snowpit profiles; (7) establishment of a network of automatic weather stations (AWS) to monitor weather conditions, local energy balance, and snowfall events in different climatic zones on the ice sheet; (8) investigation of processes associated with surface melting, from measurements taken along a transect through the ablation zone near the west coast of the ice sheet, and from satellite estimates of albedo; (9) investigation of near-surface processes associated with surface melting, ice layer formation, hoarfrost formation, and total snow accumulation rate in order to improve our ability to infer these parameters from satellite data; and (10) investigations of individual glaciers and ice streams using satellite SAR interferometry for ice velocities, core data for snow accumulation rates, and aircraft measurements of ice thickness and surface topography.

Figure 1 shows how these activities relate to the PARCA goal of quantifying and understanding the mass balance of the ice sheet, and Foldout 1 shows locations on the ice sheet where most of the associated measurements were made. Year 1999 was a milestone year for PARCA, with completion of aircraft resurveys to provide very accurate measurements of changes in surface elevation over a 5-year period for the entire ice sheet, completion of the ice coring, and significant advances in other aspects of the program. Since then, emphasis has shifted to analysis of the data, with new measurements focused on addressing important problems revealed by the analysis.

4. Key Findings

An important result from PARCA is significant improvement in our knowledge of the ice sheet mass balance. The laser- and radar-altimeter results, and those from comparison of inland snow accumulation with ice discharge across a traverse around the ice sheet, show that taken as a whole, high-elevation parts of the ice sheet are in balance to within about 1 cm/yr [*Thomas et al.*, this issue]. In contrast, most of the coastal regions of the ice sheet thinned quite rapidly during the 1990s, with net losses from the ice sheet sufficient to raise global sea level by about 0.13 mm/yr, or about 8% of the total observed rise [*Krabill et al.*, 2000]. Although coastal summer temperatures have increased recently, particularly along the east coast, the increase cannot explain observed thinning rates of up to several meters per year. This suggests that discharge velocities must also have increased. On the basis of these observations, PARCA focus has shifted to the coastal regions, with emphasis on surface ablation and its sensitivity to summer warming and possible albedo feedback, and on the dynamics of those glaciers that are observed to be changing rapidly.

We have made major advances in the application of SAR data to ice sheet research, including discovery and mapping of a major ice stream in the northeast of the ice sheet, which penetrates for hundreds of kilometers almost to the ice sheet summit [*Fahnestock et al.*, 1993]. Velocities on this, and other glaciers, have been inferred from interferometric analysis of SAR data [*Joughin et al.*, 1995; *Rignot et al.*, 1995; *Joughin et al.*, 1996a, 1998; *Rignot*, 1996; *Rignot et al.*, 1997], and grounding lines of glaciers flowing into the sea have been mapped to reveal their migrations over time [*Rignot*, 1996, 1998].

Observations of vertical crustal motion at two coastal sites show subsidence rather than the anticipated uplift [*Wahr et al.*, this issue]. For this signal to be an elastic response to recent loading would require very high values of ice thickening, far higher than observed, suggesting that the subsidence is a delayed response to earlier changes of the ice sheet significantly different from those in current models. Observed subsidence in the west suggests that the local ice sheet may have undergone a significant advance over the last 2000–3000 years. However, our available time series is short, and we estimate that at least another 5 years of observations will be required to address these issues rigorously.

Ice thickness has been successfully measured along all the aircraft flight lines, with results available within a few months of acquisition to any interested investigator [*Gogineni et al.*, this issue]. These measurements are essential requirements for all studies of ice discharge fluxes from the entire ice sheet, and from individual ice drainage basins. They are important to most PARCA investigations and are an essential boundary condition for numerical modeling studies of the ice sheet. To this end, new 5 km resolution ice thickness and bed elevation grids have been produced for the whole ice sheet by combining data collected during the 1970s and PARCA ice thickness measurements [*Bamber et al.*, this issue]. Radar sounding is also used to map internal layers in the ice sheet, indicative of past dynamics and basal conditions, and a higher-frequency radar has been used to map near-surface layers to infer snow accumulation rates [*Kanagaratnam et al.*, this issue]. Further development of this approach is directed toward an airborne shallow-depth sounder capable of tracking the depths of volcanic layers between ice core sites, and thus inferring spatial and temporal variability of snow accumulation rates over large regions.

Analysis of core data has yielded significant improvement in our knowledge of snow accumulation over the ice sheet and indicates that interannual variability of snow accumulation rates can explain at least some of the patterns of thickening and thinning observed in central parts of the ice sheet [*McConnell et al.*, 2000a]. On the basis of this finding we have used the core data to help bridge the time gap between the 1978–1988 radar altimeter surveys and the 1993–1998 laser surveys of the southern half of the ice sheet [*Thomas et al.*, 1999], and we plan to apply a similar approach to merging radar and laser measurements with future ICESAT data to compile a long time series of thickening/thinning rates for the entire ice sheet.

Initial and temporally limited (11 years) comparisons between observations and model estimates of snow accumulation show a potential link between the North Atlantic Oscillation (NAO) and the accumulation rates [*Bromwich et al.*, 1999]. The annual accumulation histories reconstructed from PARCA cores contain a climate signal, but it is masked partially by glaciological processes [*van der Veen and Bolzan*, 1999] which make extraction of a longer NAO history more difficult. Initial ice core-NAO investigations [*Appenzeller et al.*, 1998; *Barlow et al.*, 1993] were based on a single core, and although provocative have not garnered broad scientific acceptance [*Schmutz et al.*, 2000]. The PARCA cores, with their accurate dating, broad spatial distribution, and multiproxy time series, offer the best opportunity to confirm or refute the potential of Greenland ice cores for reconstruction of NAO and other oscillatory systems that dominate the Arctic climate regime.

Although NAO reconstruction is an important climate issue, the overarching PARCA goal is to assess the Greenland mass balance, both in the past and in the future. Model-based simulation of the spatial and temporal variability of precipitation shows promise, particularly when constrained by the assimilation of measurements from key locations, and offers the possibility of monitoring future spatial and temporal accumulation variability by model data assimilation of a few core data from key locations.

The network of automatic weather stations on the ice sheet is now almost complete and is routinely providing measurements of meteorological conditions, including accumulation rate, in near real time to many scientists studying a broad spectrum of research problems. These data will also be important to the interpretation of ICESAT and other satellite measurements. On the basis of the AWS data, a new annual mean air temperature map was produced [*Steffen and Box*, this issue]. The annual mean air temperature was found to be 2°C warmer for the central part of Greenland based on our AWS record for the time period 1995 to 1999, compared to the standard decade 1951 to 1960 [*Ohmura*, 1987]. This temperature increase is significant, but the timing of the warming cannot be assessed because of the limited time span of the AWS data set. Warming decreases with elevation to ~1°C for the elevation range 1000–2000 m, and this pattern of warming was predicted with high-resolution global circulation model runs for CO_2 doubling by *Ohmura et al.* [1996]. The net sublimation was also derived on the basis of the AWS data for the entire ice sheet; the total loss is on the order of 0.5×10^{14} kg, or 10% of the annual precipitation [*Box and Steffen*, this issue]. Regions most sensitive to sublimation in terms of the surface mass balance are the ablation zone and sites with small accumulation rates in the north of the ice sheet.

Significant progress is being made toward understanding microwave signatures of the ice sheet. These are strongly affected by conditions beneath the surface and contain information on depth hoar and ice layer intensity, snow temperatures and wetness, and accumulation rate. As a result of PARCA investigations, we now have a better physical understanding of how these processes affect the microwave signatures, with the prospect of more reliable techniques for extracting information from them. At present, we have most confidence in our mapping of summer melt zones derived from time series of passive-microwave data, and this shows an increasing tendency since data were first acquired in 1978, with a sharp decrease associated with the Mount Pinatubo eruption in 1991 [*Abdalati and Steffen*, 1997a, 1997b, this issue].

5. Improved Techniques for Ice Sheet Research

Before PARCA began in 1995, NASA research on the Greenland ice sheet was centered around the development and testing of new techniques for glaciological research: aircraft laser altimetry; ice depth sounding using a coherent radar; velocity mapping from SAR interferometry; and ice surface characteristics from satellite microwave data. This work continued within PARCA, and this section presents brief summaries of some of these techniques.

5.1. Ice Sheet Mass Balance

Four different approaches were applied by PARCA to infer the mass balance of the Greenland ice sheet: a conventional comparison of total snow accumulation with ice discharge; repeated surveys by precise airborne laser altimetry; time series of satellite radar-altimetry measurements; and point measurements of elevation change made down shallow bore holes.

5.1.1. Traverse around the ice sheet. During 1993–1997, ice discharge velocities were measured by repeat GPS measurements at stations ~30 km apart, completely circumnavigating the ice sheet close to the 2000-m contour [*Thomas et al.*, 1998, 2000a]. Seaward ice discharge across this traverse was compared to total upstream snow accumulation to give estimates of average thickening/thinning rates for individual large catchment basins and for the entire central part of the ice sheet. In addition to the first "volume budget" assessment of the mass balance of any large ice sheet, this work provides a wealth of information on ice velocities and their spatial variation around the entire central portion of the ice sheet.

5.1.2. Aircraft laser altimetry. Airborne laser altimetry is an application of GPS, inertial navigation, and laser ranging to produce accurate and dense measurements of topography [*Krabill et al.*, 1995]. Precise laser ranges to the surface below the aircraft are converted to vectors via attitude measurements from an inertial navigation system. These are referenced to Earth center-of-mass coordinates through postflight kinematic GPS determination of the trajectory of the aircraft. In our application the laser ranges are scanned to provide a swath of data, typically 140–250 m wide, facilitating repeated measurements separated by days or years. Aircraft guidance is derived from real-time GPS positioning. Over the past 10 years our overall capability has improved, such that in our most recent field trip to Greenland we achieved sub-10-cm repeatability over flight lines of several hundred kilometers.

Estimates of elevation change can be made by comparing the elevations of individual footprints, from different flights, which lie within a prescribed horizontal separation (typically 1 m), and this is done for areas where the surface is rough or crevassed. However, most of the ice sheet is sufficiently smooth and flat to be well described as a series of 70-m-diameter plane surfaces, or "platelets," fitted to the data. Data from different flights are compared by seeking any platelet from the second flight with its center lying close (typically within 75 m) to the center of a platelet from the first flight and by comparing heights that have been interpolated to the point midway between the two platelet centers by taking account of the platelet slopes. The RMS fit of the numerous separate laser shots to these platelets is typically 5 cm or better, and for most purposes, the platelets adequately represent the information contained within the laser data, and they enormously reduce the data volume.

5.1.3. Satellite radar altimetry. Changes in the surface elevation of the polar ice sheets have been measured using time series of surface elevations obtained from satellite radar altimeters [*Zwally et al.*, 1989]. Data from Seasat (1978) and Geosat (1985–1989) provided coverage up to ±72° latitude. Radar altimeters aboard the ERS-1 and ERS-2 satellites extended coverage to ±81.5°, with a continuous time series of data since July 1991. The NASA Ice Sheet Altimeter Pathfinder program has reprocessed these data using a consistent set of environmental corrections and orbit solutions. Early ice sheet change studies using Seasat and Geosat altimeter data suffered from a variety of problems because these instruments were never intended for this application. With progressive improvements in orbit computation [*Tapley et al.*, 1996], orbit-error analysis and reduction [e.g., *Yoon*, 1998; *Davis et al.*, 2000], ice sheet retracking [*Davis*, 1997], and identification of measurement-system biases [e.g., *Davis et al.*, 2000], ice sheet satellite radar altimetry has now evolved to a sufficient state of maturity that regional changes in surface elevation can be inferred with an accuracy on the order of a few centimeters per year over periods of 5–10 years [*Davis et al.*, 1998; *Wingham et al.*, 1998; *Zwally et al.*, 1998; *Davis et al.*, 2000]. However, errors can increase because of temporal changes in the radar-backscatter characteristics of the surface snow. Moreover, because of the large radar "footprint" and poor tracking near the ice sheet margin, reliable elevation-change estimates can be acquired only over an ice sheet with surface slopes less than about 1°.

5.1.4. Local rates of ice sheet thickness change. Local rates of ice thickness change have been measured at 11 sites on the ice sheet using precise GPS surveys. The method entails comparing the vertical component of ice velocity, as measured using GPS surveys of markers anchored at various depths in firn, with the local, long-term rate of snow accumulation from core stratigraphy [*Hamilton and Whillans*, 2000]. Adjustments are made to the vertical velocities to account for vertical motion due to along-slope flow and firn compaction. The difference between the adjusted vertical velocity and the accumulation rate is the rate of ice sheet thickness change. The results apply to timescales on the order of decades to centuries, as defined by the length of the accumulation rate records. The assumption is that ice dynamics do not change over the same time interval, which is reasonable for the interior portions of the ice sheet where the measurements were made. While the results apply locally, they represent averages over longer time periods, and comparison with regional mass-budget estimates from the traverse (section 5.1.1) gives an indication of spatial variability of ice thickening/thinning rates.

5.2. Ice Depth Sounding and Layer Tracking

The University of Kansas coherent radar depth sounder operates at a center frequency of 150 MHz [*Gogineni et al.*, 1998]. The transmitter generates a pulse of 1.6 μs duration and about 100 W peak power, which is frequency-modulated over a bandwidth of 17 MHz. It uses two antennas mounted under the left and right wings of the aircraft: one for transmission and the other for reception. Each antenna is a four-element dipole array with two-way beam widths of 18° and 66° in planes perpendicular and parallel to the flight path, respectively. The receiver amplifies and compresses the received signals in a weighted surface acoustic wave compressor to an effective pulse length of about 60 ns, resulting in a depth resolution of about 4.5 m in ice. The compressed signal is coherently detected and integrated by summing consecutive pulses. This serves as a low-pass filter and reduces the along-track antenna beam width. The pulse compression and coherent processing are the features that make this system unique and capable of sounding outlet glaciers and ice sheet margins. Good ice thickness data were collected over 90% of the PARCA flight lines [*Gogineni et al.*, this issue]. To estimate errors, the radar-determined ice thickness information was compared with GISP and GRIP cores. The results show that radar-determined ice thicknesses are within ±10 m of those at the core sites. Radar data also show continuous internal layers to a depth of about 2.5 km for 3-km-thick ice over a distance of several hundred kilometers, and these were used in support of the North Greenland Ice Core Project (NGRIP) drill site selection [*Dahl-Jensen et al.*, 1997]. Radar data were also used to determine surface roughness and echo strength at the ice-bedrock interface [*Allen et al.*, 1997].

An ultrawideband radar operating over the frequency range from 170 to 2000 MHz was developed for high-resolution mapping of internal layers in the top 200 m of ice for determining the average long-term accumulation rate. A surface-based experiment using this system was performed at the NGRIP drill site during August 1999, and data were collected over a 10-km transect. The results show that radar-determined depths to internal layers were within ±2 m of those from an ice core [*Kanagaratnam et al.*, this issue].

5.3. SAR Interferometry

Since first used to measure ice motion by *Goldstein et al.* [1993], satellite radar interferometry (SRI) has emerged as a major new tool for measuring ice motion over large, featureless areas, at high resolution, and with a uniform sampling scheme. Many advances in SRI have been made as part of PARCA investigations in Greenland, including the first measurements of ice sheet flow [*Joughin et al.*, 1995; *Rignot et al.*, 1995], ice sheet surface topography [*Kwok and Fahnestock*, 1996; *Joughin et al.*, 1996b], vector motion from crossing orbits [*Joughin et al.*, 1998; *Mohr et al.*, 1998], and grounding-line position and migration with time [*Rignot*, 1996, 1998]. These investigations benefited from the large volume of SAR data collected by the European Space Agency ERS-1 and ERS-2 satellites. SRI-derived velocities, combined with ice thickness data from the University of Kansas radar sounder, have provided significantly improved estimates of ice discharge from the large outlet glaciers that fringe the perimeter of Greenland and control its mass discharge [*Rignot et al.*, 1997; *Joughin et al.*, 1999a]. In particular, these measurements showed that basal melting of glacier floating ice tongues is a dominant process of mass ablation in the north [*Rignot et al.*, 1997] and that discharge of the northeast sector of the ice sheet is controlled by a previously unmapped 600-km-long ice stream reminiscent of those encountered in West Antarctica [*Joughin et al.*, 1999b, this issue]. The SRI techniques developed under PARCA for Greenland are now employed to study the Antarctic ice sheet and have already led to a number of important discoveries.

5.4. Ice-Surface Characteristics From Satellite Data

Early PARCA airborne and in situ observations better defined relationships between spaceborne microwave radar data and glaciological processes. For example, distinctive morphologies of the wet, percolation, and dry snow zones were used to understand large-scale tonal patterns evident across the ERS SAR mosaic [e.g., *Zabel et al.*, 1995]. These observations led to

two developments. First, better ability to interpret spaceborne imagery has improved mapping of the Greenland ice sheet margins and, using a combination of techniques, Jakobshavn Glacier was shown to have systematically retreated over the past 150 years [*Sohn et al.*, 1998]. Second, better understanding of microwave scattering from dry snow led to the development of algorithms for estimating accumulation rates from passive-microwave and SAR data [*Forster et al.*, 1999].

5.4.1. Summer melt-zone mapping. A marked change in microwave emission characteristics during the onset of melt allows for the classification of wet and dry snow based on passive-microwave brightness temperatures from the SMMR and SSM/I instruments. A single-channel approach using 37 GHz horizontal brightness temperatures provides details on the day-to-day variability of surface melt characteristics [*Mote and Anderson*, 1995]. A multichannel approach using the 19 GHz horizontal polarization combined with the 37 GHz vertical polarization has also been used [*Abdalati and Steffen*, 1997a]. This is a higher-inertia signal that dampens some of the day-to-day variability, and it is well suited to longer-term monitoring such as on seasonal and interannual scales. Currently, the methods are binary in nature, in that the firn can be classified either as wet or dry, but the different temporal inertia of the two methods shows potential for more quantitatively describing the degree of wetness. Moreover, progress is being made in combining these binary melt estimates with positive degree-day probability distributions to estimate ablation rates for some parts of the ice sheet [*Mote*, 2000]. In addition, the annual extent of melt, the melt duration, and the length of the melt season for 1979–1997 [*Joshi*, 1999] were inferred using an edge-detection algorithm applied to passive-microwave time series. The new information on melt duration and length of melt season were better related to global temperature trends than melt extent alone, largely because of the ephemeral nature of melt along transition zones between percolation and dry snow facies. Such analyses are preliminary, but they provide a significant first step toward quantitatively estimating ablation rates from passive-microwave satellite data. These methods will be applicable to the upcoming Advanced Microwave Scanning Radiometer (AMSR) scheduled for launch on the NASA AQUA mission early in 2001, which will have a spatial sampling interval (12.5 km), half that of SSM/I.

Other instruments that can be used for melt-zone mapping include SAR [*Fahnestock et al.*, 1993], wind scatterometer [*Drinkwater and Long*, 1998; *Long and Drinkwater*, 1999], and visible sensors such as advanced very high resolution radiometer (AVHRR). SAR and scatterometer methods rely on differing radar backscatter characteristics among wet, dry, and refrozen snow, while methods using visible sensors are based on reflectance properties and provide additional information about the radiant energy exchanges. Both SAR and AVHRR offer means of mapping melt/ablation characteristics at higher resolution, but SAR has limited temporal coverage, and visible sensors are limited by cloud cover, which can result in substantial gaps in coverage. These data can also be expensive and require considerable computational resources. Scatterometers such as SeaWinds onboard QuikScat and ADEOS 2 are proposed by *Long and Drinkwater* [1999] as the most suitable alternative, as they provide daily, ice sheet wide coverage at a spatial resolution of about 4.5 km. The potential also exists for combining observations from passive microwave, scatterometer, SAR, and visible imagery for a more complete description of the ice sheet melt characteristics.

5.4.2. Accumulation rates from satellite microwave data. Accumulation rates in dry snow zones can now be estimated in several different ways using satellite observations of microwave emission and backscattering. An empirical method has been published by *Bolzan and Jezek* [2001], who showed that annually averaged brightness temperatures at 19 and 37 GHz correlate very strongly with annual accumulation (and likewise for multiyear-averaged measurements) in a 150 km × 150 km region around the Greenland summit. A second empirical method, proposed by *Drinkwater et al.* [this issue], uses radar scatterometer image data from Seasat, ERS-1 and ERS-2, NSCAT, and QuikScat. On the basis of a strong Ku-band relationship between the rate of decrease in backscatter coefficient with incidence angle, snow accumulation retrievals are made possible in the dry snow zone. The observed relationship appears to be determined by the covariance of density, grain size, accumulation rate, and incidence-angle, and thus path-length-integrated volume-scattering effects in the upper layers of firn. Retrieval errors using this technique are less than 5% when compared with maps synthesized from in situ data. Decadal changes in dry-snow zone accumulation are inferred using differences between image data collected in 1978 and 1996.

A more physical method by *Zwally and Giovinetto* [1995] is based on the covariance of emissivity at 19 GHz with accumulation rate, and judicious blending of historical ground-based observation. The emissivity/accumulation rate covariance is explained as being due to physical relationships between snow-grain size and both accumulation rate and emission, but regionally dependent (empirical) adjustments in the emissivity/accumulation rate parameterization are required. Root-mean-square retrieval errors for this method in the dry-snow zone in Greenland are roughly 10%. A fourth method has been developed by *Winebrenner et al.* [this issue] based on covariance of fine-scale (of the order of 0.5 cm) density layering and accumulation rate and on the effect of layering on the polarization of emission at 6.7 GHz. While the latter effect is quantitatively understood, the layering/accumulation rate covariance is, as of this writing, only incompletely understood, and must be specified with the aid of ground-based data. In the case of Greenland, retrieval errors for this method, as judged by comparison with maps compiled from ground data, are approximately 10%. Finally, J. Munk et al. (unpublished data, 2001) use radiative transfer theory, coupled with a snow metamorphosis model, to predict backscatter as a function of accumulation rate.

5.4.3. Surface temperature and albedo mapping. Snow surface temperature and albedo can be derived from thermal and visible satellite imagery under clear skies provided a correction for the intervening atmosphere is made. Further corrections are typically needed for the derivation of surface albedo, such as a correction for directional effects and conversion from narrowband visible and near-infrared albedos to a broadband albedo. Surface temperature and albedo maps over Greenland have been previously computed using AVHRR data from 1989 to 1993 [*Stroeve and Steffen*, 1998; *Stroeve et al.*, 1997]. A more extensive time series of surface albedo and temperature for the polar regions is now available from the AVHRR Polar Pathfinder (APP) Data. Spanning the period from 1981 to 1998, gridded maps of surface albedo and temperature at a 5-km spatial resolution are available for both hemispheres. In the near future, data from the Moderate-Resolution Imaging Spectroradiometer (MODIS) will also be available for monitoring the spatial and temporal variations of


270°
280°
290°
300°
310°
320°
330°
340°
350°
0°
10°
80°
70°
60°
Humboldt [ ]
Thule
GITS [ ]
NASA_U [ ]
Crawford Point [ ]
Swiss Camp [ ]
Kangerlussuaq
DYE-2 [ ]
South Dome [ ]
TUNU [ ]
NGRIP [ ]
NASA_E [ ]
Summit [ ]
Saddle [ ]
1993&1998 laser/radar flights
1994&1999 laser/radar flights
1995 laser/radar flights
1996 laser/radar flights
1997 laser/radar flights
Named field camps
Crustal motion sites
Shallow cores (<50m)
Intermediate cores (>50m)
Local dh/dt sites
Automatic weather stations
Coastal weather stations
Ablation transect
GPS velocity stations

surface albedo and temperature over Greenland. Improved accuracy is expected, along with better cloud detection.

Extensive intercomparison between the Greenland Climate Network (GC-Net) in situ measured surface albedo and that from the APP data set has been carried out. Using data from January 1997 to August 1998, it was determined that the APP-derived surface albedos are on average 10% less than those provided by GC-Net. However, a positive bias of about 4% is observed in the in situ measurements, which would reduce the difference between the two measurements to ~6%. Since surface albedo controls the amount of solar energy available for absorption by the snowpack and is therefore closely linked with surface melt, it is important that it be monitored accurately. Further work is needed to reduce the errors in the satellite estimates.

Limited comparisons between AVHRR-derived surface temperature and that measured at the equilibrium line altitude (69.5°N, 49.3°W) were carried out during 1990 and 1991 [*Stroeve and Steffen*, 1998]. Results from this study revealed that the surface temperature could be derived to an accuracy of less than 1 K during summer. Further comparisons in time and space are needed, particularly with the APP-derived surface temperature maps.

Observations of microwave emission at 6.7 GHz (4.5-cm wavelength) can also be used to estimate mean near-surface temperature in dry-snow zones. The relatively long, 4.5-cm wavelength emission originates from depths down to ~80 m and thus is little affected by seasonal temperature variations. Fine-scale (of the order of 0.5 cm) density layering in the snow affects both the polarization of emission (which is directly observable) and the effective emissivity (which is not) in such a way as to allow accurate estimation of emissivity from polarization [*Winebrenner et al.*, this issue]. The combination of emissivity and observed brightness temperature thus yields an estimate of the 10–80 m firn temperature, which closely approximates the mean surface temperature.

5.4.4. Snow facies from satellite microwave data. *Long and Drinkwater* [1994, 1999] find Ku-band and C-band satellite-scatterometer images to be extremely effective for delimiting distinctive characteristics, or "facies" of near-surface snow. This is associated with the sensitivity of microwaves to the physical characteristics of the snow and firn in the top few meters, and the large-scale coverage of satellite radar images. The primary characteristics apparent in microwave radar data are indicative of the occurrence, intensity, and duration of summer melting as well as the seasonal metamorphosis of the firn. Summer surface melting creates stratification and distinctive changes which have a dominant impact on the scattering characteristics, particularly in the percolation zone. Refreezing of downward percolating meltwater leads to permanent buried ice lenses and ice pipes which produce extremely intense backscattering in winter. This typically leads to seasonal backscatter coefficients close to and exceeding 0 dB [*Drinkwater et al.*, this issue]. Within central Greenland the dry-snow zone is one of much lower backscatter, and a sharp spatial gradient in backscatter marks the boundary between the percolation zone and the dry snow. At higher elevations the surface experiences no melting, and this region exhibits the least seasonal variability in backscatter. At the lowest elevations, within the ablation zone, the snow cover is entirely melted to produce runoff in summer. *Drinkwater et al.* [this issue] determine the extent of this zone by summing the areas of the percolation and dry-snow zone and subtracting them from the Greenland land mask. The results of facies mapping appear consistent with previous findings of other investigators using SAR data [*Jezek et al.*, 1994; *Fahnestock et al.*, 1993]. Time series data from C-band and Ku-band radar scatterometers currently provide the most convenient data source for studies of snow facies and their changes with time.

5.5. Automatic Weather Station (AWS) Network and Meteorological Observations on the Ice Sheet

The Greenland Climate Network (GC-Net) was established in spring 1994 with the objective of monitoring climatological and glaciological parameters at various locations on the ice sheet over a time period of at least 10 years [*Steffen et al.*, 1996]. The Summit AWS in this network continues observations begun in support of the GISP2 project in 1987 [*Shuman et al.*, 2000]. The network consists of 18 stations with a distributed coverage over the Greenland ice sheet (Figure 1). Four stations are located at high elevations (~3000 m) along a north-south direction, ten stations lie close to the 2000-m contour line, and four stations are in the ablation region between 300 and 800 m elevation. Each AWS measures 32 parameters, including temperature, humidity, wind speed and wind directions at two levels, shortwave incoming and reflected radiation, net radiation, snow height, pressure, snow temperature profile from 0- to 10-m depth, GPS time, and location. Potential applications are verification of satellite-derived surface albedo; boundary conditions for ice core chemical transfer models; comparison with model analyses; coastal versus inland climate comparison; calculation of blowing-snow flux, evaporative mass flux, and surface energy balance; and logistic support for research camps on the ice sheet [e.g., *Steffen*, 1995]. Some of these applications are addressed in this issue.

5.6. Multiparameter Core Analysis

Firn and ice cores have the potential to provide annual-layer thicknesses that are the best available representations of the net annual accumulation. These annual-accumulation data reflect a combination of both the larger-scale climate signal and the local glaciological noise at the drill site. The PARCA ice-coring initiative has resulted in an impressive collection of shallow to intermediate-length cores (totaling ~2100 m) from about 60 Greenland locations. All cores cover recent decades, eight records extend back at least 250 years, and one record includes annually resolved accumulation back 800 years. Table 1 in the work of *Mosley-Thompson et al.* [this issue] contains the basic information for each PARCA core. The strength of this data set is the dating precision. The development of a continuous flow analysis system [*Fuhrer et al.*, 1993; *Anklin et al.*, 1998] has made it possible to measure simultaneously multiple chemical species such as hydrogen peroxide, calcium, ammonium, and nitrate. Some of these species exhibit seasonal concentration variations and when coupled with the seasonal variations of insoluble dust and oxygen isotopic ratios ($\delta^{18}O$), both measured in discrete samples, the dating precision is increased significantly. In many cases the PARCA cores have no dating error. This is often confirmed by the identification of beta radioactivity horizons [see *Mosley-Thompson et al.*, this issue, Figure 5] associated with known atmospheric thermonuclear tests (e.g., 1952 and 1963) and/or identification of explosive volcanic events such as Laki (1783–1984) or Tambora (1815) by excess sulfate concentration [see *Mosley-Thompson et al.*, this issue, Figures 2 and 4; *Mosley-Thompson et al.*, 1993, Figure 10]. Identification of the annual layers, coupled with the

density, allows construction of records of net annual mass accumulation [*McConnell et al.*, this issue], providing critical information to other PARCA investigations designed to address the past and present mass balance of the Greenland ice sheet.

5.7. Calculations of Accumulation Rates From Atmospheric Analyses

Observations of precipitation over Greenland are limited to the coastal regions and have large uncertainties. By contrast, the analyzed wind, geopotential height, and moisture fields for the free atmosphere over the ice sheet are available for recent years from atmospheric analyses, and this information has been used to retrieve precipitation over Greenland using a dynamic method. Results for 1985–1996 and their seasonal and interannual variations were initially related to the North Atlantic Oscillation (NAO) index [*Chen et al.*, 1997; *Bromwich et al.*, 1999]. If the NAO index increases, the precipitation over southern and western Greenland decreases, and vice versa. The correlation coefficient between these two series for the winter of 1985–1995 is −0.60 to −0.80. Newly measured time series of recent accumulation from ice cores reported for 11 sites located near the 2000-m contour of the Greenland ice sheet have been compared to retrieved precipitation covering the same time range of 1985–1995. Good agreement in their interannual variations has been found if the retrieved precipitation values at individual sites are scaled up by a fixed amount [*McConnell et al.*, 2000b]. However, *Hanna et al.* [2001] found excellent agreement between the PARCA ice core measurements and snow accumulation derived from the European Centre (ECMWF) analyses without the need for scaling. For subseasonal observations the modeling data appear to require a similar fix, estimating ~56% of the observed net accumulation but with good agreement in the annual accumulation pattern [*Shuman et al.*, this issue]. More troubling is the introduction of accumulation gradients in the model output where none appear to exist in reality.

On the basis of evaluation of recent Greenland precipitation studies [*Bromwich et al.*, 1998], several of the deficiencies in the precipitation spatial distributions are probably related to the topographic data initially employed in the modeling. The impact of using the modern topographic data set of *Ekholm* [1996], to replace the inaccurate U.S. Navy 10 arc min data set used initially, shows that some deficiencies of the retrieved precipitation are improved. The topographic effect on precipitation can be more accurately modeled by using a separation of the horizontal pressure gradient force in sigma coordinates into its irrotational and rotational parts, which are expressed by the equivalent geopotential and geo-stream-function, respectively [*Chen and Bromwich*, 1999]. This procedure is used to enhance the dynamic method, yielding improved agreement between the interannual variations observed in accumulation from ice cores and those found from the dynamically retrieved precipitation. No adjustment of retrieved precipitation amounts is now needed.

Accumulation estimates from the ice cores provide detailed information on temporal variability, but this is partly obscured by spatial noise from surface irregularities [*van der Veen and Bolzan*, 1999], such as sastrugi and undulations [see *Mosley-Thompson et al.*, this issue, Figures 6 and 7]. This spatial noise must be estimated and removed from ice core records for reliable descriptions of temporal variability to be obtained. Collection of several duplicate cores separated by 10 s of kilometers allows this spatial noise to be averaged out and provides spatially averaged temporal variability on a length scale that approaches that resolved by the precipitation calculations. The best set of such cores was collected at Humboldt [*Mosley-Thompson et al.*, this issue], where low accumulation enhances the significance of spatial variability. It is desirable to collect such multiple cores in a contemporary sampling of all four major ice sheet environments (south, western, central, and north) for testing and calibration of retrieved precipitation amounts. When completed, such an effort would not need to be repeated, and only a very limited coring program would be desirable to check ongoing precipitation calculations.

6. Research Highlights

6.1. Improved Accumulation From Cores

Accurate spatial estimates of snow accumulation on the Greenland ice sheet are a central ingredient in essentially all studies of ice sheet mass balance. Recent PARCA and European cores have approximately doubled the number of years of accumulation records over the ice sheet and addressed many of the previous uncertainties in accumulation. This is because most PARCA cores cover at least two decades, and most older point measurements were for fewer than 10 years. PARCA results show that accumulation in the west central part of the ice sheet is considerably less than previously thought [*Bales et al.*, this issue], and there are regions with higher, and others with lower, values for the southern portion. However, the total accumulation for the entire ice sheet is almost identical to that based on the earlier, sparser data.

6.1.1. Accumulation and NAO. The spatially distributed records of accumulation from the PARCA cores also provide an excellent index of how large-scale circulation influences Greenland climate. Over the past 130 years, approximately one third of the observed variability in annual accumulation from PARCA cores in the northwestern part of Greenland can be linked to the North Atlantic Oscillation (NAO) [*Bales et al.*, this issue]. The deeper PARCA cores from west central and northwest Greenland, which cover several centuries, offer the potential for development of a proxy NAO history and the opportunity to improve the initial efforts by *Appenzeller et al.* [1998] on the basis of a single ice core record. Preliminary data suggest that cores farther inland show a weaker correlation with NAO indices. Perhaps the best promise for understanding how NAO and related large-scale phenomena influence regional accumulation on the ice sheet will come from a more detailed analysis of the accumulation records, establishing spatially averaged accumulation variations on a year-by-year basis [*McConnell et al.*, this issue].

6.1.2. Temporal variability in snow accumulation and surface-elevation changes. While repeat altimetry surveys over southern Greenland show little overall elevation change at higher elevations, they show large spatial variability [*Davis et al.*, 1998; *Zwally et al.*, 1998; *Krabill et al.*, 1999]. In particular, significant thickening was observed to the west of the ice sheet elevation divide below ~68°N and rapid thinning to the east. Taken alone, these altimetry studies were unable to determine the underlying geophysical processes (e.g., changing snow accumulation, increased basal slip) driving current ice sheet elevation change, nor to assess if current rates of change exceed the natural variability. To address these issues, *McConnell et al.* [2000a] used widely distributed records of annual snow accumulation from ice cores and a physically based model of snow

densification [*Arthern and Wingham*, 1998] to derive the 1978–1988 ice sheet elevation change (dH/dt) resulting solely from measured variability in snow accumulation (dA/dt). While error analyses indicate that uncertainty in accumulation-driven dH/dt arises primarily from well-documented spatial variability in snow accumulation, overall uncertainties were generally smaller than the estimated dH/dt. Because accumulation-forced dH/dt was in close agreement with observed dH/dt from Seasat/Geosat satellite altimetry at 11 of 12 locations studied, the majority of the 1978–1988 change in ice sheet elevation above 2000 m was attributed to temporal and spatial variability in accumulation. Similar analyses using seven longer ice core accumulation records indicate that the observed 10-year changes in ice surface elevation for central parts of the ice sheet are typical of accumulation-driven dH/dt over the past few centuries. However, areas of very rapid change, particularly in the southeast, cannot be explained in this way and appear to be undergoing dynamic changes [*Thomas et al.*, this issue].

6.2. Surface Ablation

Most investigations of surface ablation have been concentrated in west Greenland in connection with the mapping of hydropower potential. More recently, measurements have been made in connection with climatology studies [*van de Wal et al.*, 1995; *Braithwaite*, 1983; *Ohmura et al.*, 1994]. Ice ablation rates of 3–4 m/yr measured on outlet glaciers are common at lower elevations in south Greenland. Along the western slope the net ablation is difficult to assess due to the wide extent of the slush zone (30–50 km wide). Automatic weather stations positioned along profiles across all glacier facies might provide crucial information in the future. The AWS station located in the ablation region along the west slope of the ice sheet at 900 m above sea level, measured an average annual ablation of 104 cm for 1996 and 1997, with summer air temperatures near the melting point and clear-sky conditions. The strong albedo feedback and, consequently, the increase in absorbed solar radiation is the major driver for the surface ablation in summer. Meltwater lakes, which are common in this elevation band all around the perimeter of Greenland, enhance the surface ablation further, owing to their lower surface albedo.

6.2.1. Melt trends. Analysis of the passive-microwave-derived melt characteristics of the Greenland ice sheet has been extended to include data from 1995 to 1999 acquired by the SSM/I F-13 instrument, increasing the melt record to 20 years. Extending the time series required matching of the F-13-derived melt characteristics to those simultaneously derived with the F-11 sensor during a several-month period of overlap. Such geophysical parameter matching is essential to account for instrumental differences and to assure consistency within the time series. Results from the longer time period spanning four instruments show an increasing melt trend for the period 1979–1999 of 0.85% per year, driven primarily by the behavior of the western side of the ice sheet. The melt demonstrates a high temporal variability and shows signs of being influenced by the eruption of Mount Pinatubo and other climatological phenomena.

6.3. Outlet Glaciers

Satellite radar interferometry (SRI) has been employed to detect glacier surges, grounding-line positions, and migration rate, and to infer ice discharge and ice shelf basal melt rates. The minisurge of Ryder Gletscher [*Joughin et al.*, 1996c] illustrated that surging glaciers are not uncommon in northern Greenland [*Higgins and Weidick*, 1988], even though summer meltwater production is limited. Glacier grounding lines mapped for the first time in north Greenland at a high spatial resolution (a few tens of meters) revealed that 3.5 times more ice flows out of this part of the ice sheet than previously estimated [*Rignot et al.*, 1997]. The discrepancy between prior and new estimates is due to extensive basal melting beneath ice shelves. The inferred basal melt rates (10–20 m/yr) are 1 to 2 orders of magnitude larger than estimates for most Antarctic ice shelves. Comparison of coastal ice discharge with mass accumulation suggests that more ice is being discharged from northern Greenland glaciers than accumulates in the interior, but the errors associated with snow accumulation and runoff remain large. On a shorter timescale, but with greater certainty, SRI measured that the grounding lines of major north Greenland glaciers (Humboldt, Petermann, Ryder, Ostenfeld, and Nioghalvfjerdbrae) retreated between 1992 and 1996 [*Rignot*, 1998; *Rignot et al.*, 2000, this issue]. The retreat rate of several hundred meters per year suggests local ice thinning at the meter per year level, which is unlikely to be caused by temporal changes in accumulation and/or ablation, implying that ice near the grounding line must be thinning by anomalously high creep. Along the southeast coast of Greenland, ice thinning is even more dramatic [*Krabill et al.*, 1999, 2000]. The first mapping of glacier velocities shows that Helheim Gletscher moves at 8 km/yr, which is faster than Jakobshavn Isbrae in west Greenland. Kangerdlugssuaq Gletscher, another fast-moving glacier, is thinning at rates increasing to 10 m/yr at the coast but with stable ice-front positions since the early 1960s and steady ice velocities until the late 1990s when the glacier apparently accelerated, probably causing the rapid thinning [*Thomas et al.*, 2000b]. A number of other glaciers draining east Greenland are also undergoing rapid thinning, possibly also caused by accelerated flow [*Abdalati et al.*, this issue].

6.3.1. Northeast ice stream. Initial work on a SAR mosaic and visible imagery revealed the presence of a large ice stream in NE Greenland which discharges ice into three major outlet glaciers along the coast. This feature reaches well into the interior, with a catchment that includes the northern side of the summit dome. A combination of interferometric analysis of ERS-1 and ERS-2 SAR data, controlled by balance velocities and GPS measurements, and ice-penetrating radar measurements, have allowed us to characterize the ice flow and basal configuration of this ice stream. The velocity map makes this ice stream the best documented in terms of surface motion and provides a rigorous boundary condition for understanding the mechanics of rapid ice flow. There are similarities between this ice stream and extensive ice streams in the interior of East Antarctica. There are also differences between this ice stream and the intensively studied ice streams of West Antarctica, most notably the larger surface slopes in Greenland, indicating a stronger interaction with the bed.

6.4. Mass Balance

PARCA results have significantly improved our understanding of the mass balance of the Greenland ice sheet. Prior to the program, we could not determine whether the ice sheet was increasing or decreasing in volume, and mass-balance errors were equivalent to about ± 10 cm/yr thickness change for the entire ice sheet. Since then, repeat surveys by satellite radar altimeter (1978–1988 and 1992–1999), and by aircraft laser altimeter (1993/1994–1998/1999), and volume-balance esti-

mates from comparison of total snow accumulation with total ice discharge show that the entire region of the ice sheet above about 2000-m elevation has been close to balance (within 1 cm/yr) for at least the past few decades but with smaller areas of quite rapid change that can largely be explained by temporal variability in snow accumulation rates. Some areas in the south, however, appear to be undergoing large changes, which may be ongoing adjustments to events since the last glacial maximum, or they may be indicative of changes that began only recently [*Thomas et al.*, this issue]. In particular, most surveyed outlet glaciers are thinning in their lower reaches [*Abdalati et al.*, this issue], and a large area of ice sheet in the southeast has also thinned significantly over the past few decades, at rates that increase to more than 1 m/yr near the coast. Only a part of this thinning can be explained by increased melting associated with recent warmer summers, indicating that ice discharge velocities must also have increased.

Continuous GPS measurements by a receiver that PARCA installed on bedrock near Kangerlussuaq show that the Earth's crust in that region is subsiding at about 6 ± 2 mm/yr [*Wahr et al.*, this issue]. This result is qualitatively consistent with archeological and historical evidence, from along the southwest coast of Greenland, which indicates varying rates of subsidence in that region over the last thousand years or so. The observed rate of subsidence is too large to be caused by the Earth's elastic response to present-day variations in nearby ice. Furthermore, models of the Earth's viscoelastic response to the thinning and deglaciation of Greenland and surrounding regions prior to 4000 years ago predict a present-day uplift, rather than subsidence, of 3–4 mm/yr. The GPS results thus show about 9–10 mm/yr of unexplained subsidence. To explain the archeological and historical measurements, it has been proposed that after several thousand years of retreat, the western margin of the ice sheet may have reversed itself and begun readvancing around 2000–3000 years ago [*Weidick*, 1993]. Our modeling indicates that depending on the details of this advance and on the Earth's viscosity profile, Kangerlussuaq could conceivably be subsiding viscoelastically in response to this advancing ice at a rate of several millimeters per year: perhaps enough to explain the GPS results.

By contrast to the overall balance at high elevations, the laser surveys reveal significant thinning along 70% of the ice sheet periphery below a 2000-m elevation [*Abdalati et al.*, this issue]. Thinning rates of more than 1 m/yr are common along many outlet glaciers, in some cases at elevations up to 1500 m. Warmer summers along parts of the coast may have caused a few tens of centimeters per year additional melting, but most of the observed thinning probably results from increased glacier velocities and associated creep rates. Three glaciers in the northeast all show patterns of thickness change indicative of surging behavior, and one has been independently documented as a surging glacier. However, we have no explanation for the widespread thinning, at all latitudes, of most surveyed glaciers. There are a few areas of significant thickening (up to 50 cm/yr), and these may be related to higher than normal local accumulation rates during the observation period. The total net thinning of the ice sheet is equivalent to a sea level rise of about 0.13 mm/yr, or almost 10% of the observed signal.

6.5. Climatology

The AWS network at its present configuration captures well the regional climate in the accumulation zone of the Greenland ice sheet. The coldest month occurs in February and the warmest month in July for all AWS sites on the ice sheet. The annual monthly mean temperature amplitude exceeds 30°C in north, northeast, northwest, and central Greenland with decreasing amplitude from north to south and with decreasing elevation. The annual mean latitudinal temperature gradient for the western slope of the ice sheet is 0.78°C/degree latitude and 0.82°C/degree for the eastern slope. Consequently, the climate at the eastern side of Greenland is colder compared to the western side at the same latitude. The mean annual lapse rate along the slope of the ice sheet is 0.71°C/100 m based on 14 AWS sites between 962 m and 3254 m.

Firn temperatures at 10 m in depth in the north and the central part of Greenland (dry-snow zone) were 1° to 2.5°C colder than the annual mean air temperature of the previous year. In the percolation zone, the 10-m firn temperature was warmer than the annual mean air temperature due to refreezing of meltwater. At the equilibrium line altitude the 10-m ice temperature depends strongly on the insulating effects of the seasonal snow cover. In general, we conclude that the 10-m firn temperature is only good within ±2°C for annual mean air temperature approximation.

The annual mean wind speed at a 2000-m elevation ranges between 4.8 and 6.9 m/s for all regions on the ice sheet. Along the west slope of the ice sheet the wind speed increases by 1% per 100-m elevation descent, and wind speed and direction are controlled by the katabatic outflow of the air masses. At higher elevations, near the top of the ice sheet, the large-scale synoptic is the dominant factor that governs the wind field.

The net surface accretion (accumulation minus sublimation) in the dry-snow region of the ice sheet can be approximated with a linear model based on monthly mean values. There is no pronounced seasonal cycle of accumulation for the northern and central part of Greenland, where monthly surface accretion is typically 0.1 m. In contrast, the seasonal accumulation cycle in the southern part of Greenland is evident with higher accumulation in late fall and early winter (October through December) and the least surface accretion in the month of May.

7. Future Directions

Approximately half of the ice lost from the Greenland ice sheet is by surface melting and runoff into the sea, with most of the rest by ice discharge and basal melting from the floating portions of outlet glaciers. By contrast, there is very little ice loss by surface melting in Antarctica. Consequently, near-coastal ice in Greenland is likely to respond rapidly and sensitively to warming climate, with an increase in both the area and the intensity of summer melting. In addition to increasing the rate of meltwater discharge into the ocean, this would also increase meltwater flow into crevasses and thence to the beds of outlet glaciers, leading to more rapid basal sliding. It has been suggested that Greenland was responsible for rapid sea level rise during the last interglacial [*Cuffey and Marshall*, 2000], so understanding the mechanisms that control the ice sheet balance and how they may respond to climate change is a high priority.

PARCA has completed the first overall assessment of the mass balance of the Greenland ice sheet, but this work represents only the reconnaissance phase of a complete study. It has shown that significant changes are taking place in coastal regions, precisely where the ice sheet should be most sensitive to climate warming. However, observed warming in these regions

is quite modest, and there is a clear need for well-focused research addressing two objectives, ablation and outlet glaciers: an ablation program to improve understanding sufficiently for development of reliable parameterizations of surface melt rates in terms of weather parameters, such as temperatures and winds, whether they are observed or derived from models, and an outlet glacier program to identify and quantify the controls over glacier motion, and to determine the sensitivity of glacier speed to perturbations in these controls.

Results from PARCA to date, together with those from studies of ablation and outlet glaciers, should provide a solid foundation for the interpretation and analysis of Greenland data from the upcoming ICESAT mission. The aircraft laser-altimeter measurements represent baseline data extending back to the early 1990s for comparison with ICESAT measurements of surface elevations wherever orbit tracks cross the PARCA flight lines. This will significantly extend the temporal coverage of our estimates of elevation change over most of the ice sheet. In addition, PARCA ice core results will help isolate regions of long-term thickness change from those where change is most likely caused by temporal variability in accumulation rates, and interpretation of observed patterns of elevation change will benefit from satellite time series of surface characteristics, AWS measurements, and the results of process studies initiated by PARCA. We strongly recommend continued efforts to maintain these activities: satellite time series should be extended to include data from new sensors, such as MODIS, AMSR, Seawinds, and GLAS; the AWS network should be optimized, based on analysis of acquired data, to remove redundant stations and perhaps to establish new stations in ablation regions; and studies addressing ablation and the dynamics of thinning glaciers should be emphasized.

Finally, we believe that the approach adopted by PARCA, a focused, yet interdisciplinary, effort strongly guided by clearly stated goals and objectives, comprising an appropriate mix of in situ and remote sensing data acquisition, interpretation, and modeling, can be applied to the ice sheet in Antarctica. This will require interagency and international collaboration, which runs the very real risk of diluting the focus and weakening the guidance. However, ICESAT and SAR data offer the opportunity for costly in situ and aircraft projects to be guided and focused by satellite detection of regions undergoing significant change.

Acknowledgments. The work presented in this special section was supported primarily by the NASA Polar Research Program but has benefited significantly from collaboration with numerous scientists, mainly from Europe, not involved in the NASA program. This level of cooperation and communication adds considerably to the enjoyment most of us have in working in Greenland. All the work was heavily dependent on logistic support, and we thank Karl Kuivinen and others from the Polar Ice Coring Office for the excellent support we received from them. Much of the work required aircraft support from ski-equipped Twin Otter aircraft, and we all benefited from the long hours of safe and reliable flying, often under difficult conditions, completed by the chief pilot Jonas Finnbogason of Greenlandair. Finally, we thank the Greenland Home Rule Government for permitting free access to the ice sheet to all interested scientists.

References

Abdalati, W., and K. Steffen, Snowmelt on the Greenland ice sheet as derived from passive microwave satellite data, *J. Clim.*, *10*, 165–175, 1997a.

Abdalati, W., and K. Steffen, The apparent effect of the Mt. Pinatubo eruption on the Greenland ice sheet melt conditions, *Geophys. Res. Lett.*, *24*, 1795–1797, 1997b.

Abdalati, W., and K. Steffen, Greenland ice sheet melt extent: 1979–1999, *J. Geophys. Res.*, this issue.

Abdalati, W., W. Krabill, E. Frederick, S. Manizade, C. Martin, J. Sonntag, R. Swift, R. Thomas, W. Wright, and J. Yungel, Outlet glacier and margin elevation changes: Near-coastal thinning of the Greenland ice sheet, *J. Geophys. Res.*, this issue.

Allen, C. T., M. Ghandi, P. Gogineni, and K. C. Jezek, Feasibility study for mapping the polar ice bottom topography using interferometric synthetic-aperture radar techniques, *Remote Sens. Lab. Tech. Rep. 11680-1*, Univ. of Kansas, Lawrence, 1997.

Alley, R. B., et al., Abrupt increase in Greenland snow accumulation at the end of the Younger Dryas event, *Nature*, *362*, 527–529, 1993.

Anklin, M., R. C. Bales, E. Mosley-Thompson, and K. Steffen, Annual accumulation at two sites in northwest Greenland during recent decades, *J. Geophys. Res.*, *103*, 28,775–28,783, 1998.

Appenzeller, C., T. F. Stocker, and M. Anklin, North Atlantic Oscillation dynamics recorded in Greenland ice cores, *Science*, *282*, 446–449, 1998.

Arthern, R. J., and D. J. Wingham, The natural fluctuations of firn densification and their effect on the geodetic determination of ice sheet mass balance, *Clim. Change*, *40*, 605–624, 1998.

Bales, R. C., E. Mosley-Thompson, and J. R. McConnell, Variability of accumulation in northwest Greenland over the past 250 years, *Geophys. Res. Lett.*, *28*(14), 2679–2682, 2001.

Bales, R. C., J. R. McConnell, E. Mosley-Thompson, and B. Csatho, Accumulation over the Greenland ice sheet from historical and recent records, *J. Geophys. Res.*, this issue.

Bamber, J. L., and R. Layberry, A new ice thickness and bed data set for the Greenland ice sheet, 1, *J. Geophys. Res.*, this issue.

Barlow, L. K., J. W. C. White, R. G. Barry, J. C. Rogers, and P. M. Grootes, The North Atlantic oscillation signature in deuterium and deuterium excess signals in the Greenland ice sheet Project 2 ice core, 1840–1970, *Geophys. Res. Lett.*, *20*, 2901–2904, 1993.

Bolzan, J. F., K. C. Jezek, Accumulation rate changes in central Greenland from passive microwave data, *J. Geophys. Res.*, in press, 2001.

Box, J., and K. Steffen, Sublimation on the Greenland ice sheet from automated weather station observations, *J. Geophys. Res.*, this issue.

Braithwaite, R. J., Detection of climate signal by interstake correlations on annual ablation data Qamanârssûp Sermia, West Greenland, *J. Glaciol.*, *35*, 253–259, 1983.

Braithwaite, R. J., Is the Greenland ice sheet getting thicker?, *Clim. Change*, *23*, 379–381, 1993.

Bromwich, D. H., R. I. Cullather, Q.-S. Chen, and B. M. Csatho, Evaluation of recent precipitation studies for Greenland ice sheet, *J. Geophys. Res.*, *103*, 26,007–26,024, 1998.

Bromwich, D. H., Q.-S. Chen, Y. Li, and R. I. Cullather, Precipitation over Greenland and its relation to the North Atlantic Oscillation, *J. Geophys. Res.*, *104*, 22,103–22,115, 1999.

Chen, Q.-S., and D. H. Bromwich, An equivalent isobaric geopotential height and its application to synoptic analysis and generalized omega-equation in sigma-coordinates, *Mon. Weather Rev.*, *127*, 145–172, 1999.

Chen, Q.-S., D. H. Bromwich, and L. Bai, Precipitation over Greenland retrieved by a dynamic method and its relation to cyclonic activity, *J. Clim.*, *10*, 839–870, 1997.

Cuffey, K. M., and S. J. Marshall, Substantial contribution to sea-level rise during the last interglacial from the Greenland ice sheet, *Nature*, *404*, 591–594, 2000.

Dahl-Jensen, D., N. S. Gundestrup, K. Keller, S. J. Johnsen, S. P. Gogineni, C. T. Allen, T. S. Chuah, H. Miller, S. Kipfstuhl, and E. D. Waddington, A search in North Greenland for a new ice core drill site, *J. Glaciol.*, *43*, 300–306, 1997.

Davis, C. H., A robust threshold retracking algorithm for measuring ice sheet surface elevation change from satellite radar altimeters, *IEEE Trans. Geosci. Remote Sens.*, *35*, 974–979, 1997.

Davis, C. H., C. A. Kluever, and B. J. Haines, Elevation change of the southern Greenland ice sheet, *Science*, *279*, 2086–2088, 1998.

Davis, C. H., C. A. Kluever, B. J. Haines, C. Perez, and Y. Yoon, Improved elevation change measurement of the southern Greenland ice sheet from satellite radar altimetry, *IEEE Trans. Geosci. Remote Sens.*, *38*, 1367–1378, 2000.

Drinkwater, M. R., and D. G. Long, Seasat, ERS-1/2 and NSCAT scatterometer-observed changes on the large ice sheets, in *Proceedings of the Joint ESA-EUMETSAT Workshop on Emerging Scatterom-*

eter Applications—From Research to Operations, ESA SP-424, pp. 91–96, ESA Publ. Div., ESTEC, Noordwijk, Netherlands, 1998.

Drinkwater, M. R., D. G. Long, and A. W. Bingham, Greenland snow accumulation estimates from satellite radar scatterometer data, *J. Geophys. Res.*, this issue.

Ekholm, S., A full coverage, high-resolution, topographic model of Greenland computed from a variety of digital elevation data, *J. Geophys. Res.*, *101*, 21,961–21,972, 1996.

Fahnestock, M., R. Bindschadler, R. Kwok, and K. Jezek, Greenland ice-sheet surface properties and ice dynamics from ERS-1 SAR imagery, *Science*, *262*, 1530–1534, 1993.

Forster, R. R., K. C. Jezek, J. Bolzan, F. Baumgartner, and S. Gogineni, Relationships between radar backscatter and accumulation rate on the Greenland ice sheet, *Int. J. Remote Sens.*, *20*, 3131–3147, 1999.

Fuhrer, K., A. Neftel, M. Anklin, and V. Maggi, Continuous measurements of hydrogen peroxide, formaldehyde, calcium and ammonium concentrations along a new GRIP ice core from Summit, central Greenland, *Atmos. Environ.*, *27*, 1873–1880, 1993.

Gogineni, S., T. Chuah, C. Allen, K. Jezek, and R. K. Moore, An improved coherent radar depth sounder, *J. Glaciol.*, *44*, 659–669, 1998.

Gogineni, S., D. Tammana, D. Braaten, C. Leuschen, T. Akins, J. Legarsky, P. Kanagaratnam, J. Stiles, C. Allen, and K. Jezek, Coherent radar ice thickness measurements over the Greenland ice sheet, *J. Geophys. Res.*, this issue.

Goldstein, R. M., H. Engelhardt, B. Kamb, and R. M. Frolich, Satellite radar interferometry for monitoring ice sheet motion: Application to an Antarctic ice stream, *Science*, *262*, 1525–1530, 1993.

Hamilton, G. S., and I. M. Whillans, Point measurements of mass balance of the Greenland Ice Sheet using precision vertical Global Positioning System (GPS) surveys, *J. Geophys. Res.*, *105*, 16,295, 2000.

Hanna, E., P. Valdes, and J. McConnell, Patterns and variations of snow accumulation over Greenland, 1979–98, from ECMWF analyses, and their verification, *J. Clim.*, in press, 2001.

Higgins, A. K., and A. Weidick, The world's northernmost surging glacier?, *Z. Gletscherk. Glazialgeol.*, *24*, 111–123, 1988.

Jezek, K. C., P. Gogineni, and M. Shanableh, Radar measurements of melt zones on the Greenland ice sheet, *Geophys. Res. Lett.*, *21*, 33–36, 1994.

Joshi, M., Estimation of surface melt and absorbed radiation on the Greenland ice sheet using passive microwave data, Ph.D. thesis, 158 pp., Ohio State Univ., Columbus, 1999.

Joughin, I., D. P. Winebrenner, and M. Fahnestock, Observations of complex ice sheet motion in Greenland using satellite radar interferometry, *Geophys. Res. Lett.*, *22*, 571–574, 1995.

Joughin, I., R. Kwok, and M. Fahnestock, Estimation of ice sheet motion using satellite radar interferometry: Method and error analysis with application to the Humboldt Glacier, Greenland, *J. Glaciol.*, *42*, 564–575, 1996a.

Joughin, I., D. P. Winebrenner, M. Fahnestock, R. Kwok, and W. Krabill, Measurement of ice-sheet topography using satellite radar interferometry, *J. Glaciol.*, *42*, 231–241, 1996b.

Joughin, I., S. Tulaczyk, M. Fahnestock, and R. Kwok, A mini-surge on the Ryder Glacier, Greenland, observed via satellite radar interferometry, *Science*, *274*, 228–230, 1996c.

Joughin, I., R. Kwok, and M. Fahnestock, Interferometric estimation of the three-dimensional ice-flow velocity vector using ascending and descending passes, *IEEE Trans. Geosci. Remote Sens.*, *36*, 25–37, 1998.

Joughin, I., M. Fahnestock, R. Kwok, P. Gogineni, and C. Allen, Ice flow of Humboldt, Petermann and Ryder Gletscher, northern Greenland, *J. Glaciol.*, *45*, 231–241, 1999a.

Joughin, I., L. Gray, R. Bindschadler, S. Price, D. Morse, C. Hulbe, K. Mattar, and C. Werner, Tributaries of West Antarctic ice streams revealed by RADARSAT interferometry, *Science*, *286*, 283–286, 1999b.

Joughin, I., M. Fahnestock, D. MacAyeal, J. Bamber, and P. Gogineni, Observation and analysis of ice flow in the largest Greenland ice stream, *J. Geophys. Res.*, this issue.

Kanagaratnam, P., S. P. Gogineni, N. Gundestrup, and L. Larsen, High-resolution radar mapping of internal layers at NGRIP, *J. Geophys. Res.*, this issue.

Krabill, W. B., and C. F. Martin, Aircraft positioning using global positioning system carrier phase data, *J. Inst. Nav.*, *34*, 1–21, 1987.

Krabill, W., R. Thomas, C. Martin, R. Swift, and E. Frederick, Accuracy of airborne laser altimetry over the Greenland ice sheet, *Int. J. Remote Sens.*, *16*, 1211–1222, 1995.

Krabill, W., E. Frederick, S. Manizade, C. Martin, J. Sonntag, R. Swift, R. Thomas, W. Wright, and J. Yungel, Rapid thinning of parts of the southern Greenland ice sheet, *Science*, *283*, 1522–1524, 1999.

Krabill, W., W. Abdalati, E. Frederick, S. Manizade, C. Martin, J. Sonntag, R. Swift, R. Thomas, W. Wright, and J. Yungel, Greenland ice sheet: High-elevation balance and peripheral thinning, *Science*, *289*, 428–430, 2000.

Kwok, R., and M. A. Fahnestock, Ice sheet motion and topography from radar interferometry, *IEEE Trans. Geosci. Remote Sens.*, *34*, 189–200, 1996.

Long, D. G., and M. R. Drinkwater, Greenland ice sheet surface properties observed by the Seasat-A scatterometer at enhanced resolution, *J. Glaciol.*, *40*, 213–230, 1994.

Long, D. G., and M. R. Drinkwater, Cryosphere applications of NSCAT data, *IEEE Trans. Geosci. Remote Sens.*, *37*, 1671–1684, 1999.

McConnell, J. R., R. J. Arthern, E. Mosley-Thompson, C. H. Davis, R. C. Bales, R. Thomas, J. F. Burkhart, and J. D. Kyne, Changes in Greenland ice sheet elevation attributed primarily to snow accumulation variability, *Nature*, *406*, 877–879, 2000a.

McConnell, J. R., E. Mosley-Thompson, D. H. Bromwich, R. C. Bales, and J. D. Kyne, Interannual variations of snow accumulation on the Greenland Ice Sheet (1985–1996): New observations versus model predictions, *J. Geophys. Res.*, *105*, 4039–4046, 2000b.

McConnell, J. R., G. Lamorey, E. Hanna, E. Mosley-Thompson, R. C. Bales, D. Belle-Oudry, and J. D. Kyne, Annual net snow accumulation over southern Greenland from 1975 to 1998, *J. Geophys. Res.*, this issue.

Mohr, J. J., N. Reeh, and S. N. Madsen, Three-dimensional glacial flow and surface elevation measured with radar interferometry, *Nature*, *391*, 273–276, 1998.

Mosley-Thompson, E., L. G. Thompson, J. Dai, M. Davis, and P. N. Lin, Climate of the last 500 years: High resolution ice core records, *Quat. Sci. Rev.*, *12*, 419–430, 1993.

Mosley-Thompson, E., J. R. McConnell, R. C. Bales, Z. Li, P.-N. Lin, K. Steffen, L. G. Thompson, R. Edwards, and D. Bathke, Local to regional-scale variability of Greenland accumulation on the Greenland ice sheet from PARCA cores, *J. Geophys. Res.*, this issue.

Mote, T. L., Ablation rate estimates over the Greenland ice sheet from microwave radiometric data, *Prof. Geogr.*, *52*, 322–331, 2000.

Mote, T. L., and M. R. Anderson, Variations in snowpack melt on the Greenland ice sheet based on passive microwave measurements, *J. Glaciol.*, *41*, 51–60, 1995.

Ohmura, A., New temperature distribution maps for Greenland, *Z. Gletscherk. Glazialgeol.*, *21*(1), 1–45, 1987.

Ohmura, A., T. Konzelmann, M. Rothach, J. Forrer, M. Wild, A. Abe-Ouchi, and H. Toritani, Energy balance for the Greenland ice sheet by observation and model computation, in *Snow and Ice Cover: Interactions With the Atmosphere and Ecosystem*, *IAHS Publ.*, *233*, 85–94, 1994.

Ohmura, A., M. Wild, and L. Bengtsson, A possible change in mass balance of Greenland and Antarctic ice sheets in the coming century, *J. Clim.*, *9*, 2124–2135, 1996.

Rignot, E., Tidal flexure, ice velocities and ablation rates of Petermann Gletscher, Greenland, *J. Glaciol.*, *42*, 476–485, 1996.

Rignot, E., Hinge-line migration of Petermann Gletscher, north Greenland, detected using satellite radar interferometry, *J. Glaciol.*, *44*, 469–476, 1998.

Rignot, E., K. C. Jezek, and H. G. Sohn, Ice flow dynamics of the Greenland Ice Sheet from SAR interferometry, *Geophys. Res. Lett.*, *22*, 575–578, 1995.

Rignot, E., S. Gogineni, W. Krabill, and S. Ekholm, Ice discharge from north and northeast Greenland as observed from satellite radar interferometry, *Science*, *276*, 934–937, 1997.

Rignot, E., G. Buscarlet, B. Csatho, S. Gogineni, W. Krabill, and M. Schmeltz, Mass balance of the northeast sector of the Greenland Ice Sheet: A remote sensing perspective, *J. Glaciol.*, *46*, 265–273, 2000.

Rignot, E., S. Gogineni, I. Joughin, and W. B. Krabill, Contribution to the glaciology of northern Greenland from satellite radar interferometry, *J. Geophys. Res.*, this issue.

Schmutz, C., J. Luterbacher, D. Gyalistras, E. Xoplaki, and H. Wanner, Can we trust proxy-based NAO index reconstructions?, *Geophys. Res. Lett.*, *27*, 1135–1138, 2000.

Shuman, C. A., K. Steffen, J. E. Box, and C. R. Stearns, A dozen years of temperature observations at the Summit: Central Greenland automatic weather stations 1987–1999, *J. Appl. Meteorol.*, in press, 2000.

Shuman, C. A., D. H. Bromwich, J. Kipfstuhl, and M. Schwager, Multiyear accumulation and temperature history near the NGRIP site, north central Greenland, *J. Geophys. Res.*, this issue.

Sohn, H. S., K. C. Jezek, and C. J. van der Veen, Jakobshavn Glacier, West Greenland: 30 years of spaceborne observations, *Geophys. Res. Lett.*, *25*, 2699–2702, 1998.

Steffen, K., Surface energy exchange during the onset of melt at the equilibrium line altitude of the Greenland ice sheet, *Ann. Glaciol.*, *21*, 13–18, 1995.

Steffen, K., and J. Box, Surface climatology of the Greenland ice sheet: Greenland Climate Network 1995–1999, *J. Geophys. Res.*, this issue.

Steffen, K., J. Box, and W. Abdalati, Greenland climate network: GC-Net, in *Glacier, Ice Sheets, and Volcanoes, CRREL Rep. 96-27*, pp. 98–103, Cold Reg. Res. and Eng. Lab., Hanover, N. H., 1996.

Stroeve, J., and K. Steffen, Variability of AVHRR-derived clear sky surface temperature over the Greenland Ice Sheet, *J. Applied Meteorol.*, *37*, 23–31, 1998.

Stroeve, J., A. Nolin, and K. Steffen, Comparison of AVHRR-derived and in-situ surface albedo over the Greenland ice sheet, *Remote Sens. Environ.*, *62*, 262–276, 1997.

Tapley, B. D., et al., The joint gravity model 3, *J. Geophys. Res.*, *101*, 28,029–28,049, 1996.

Thomas, R. H., B. M. Csatho, S. Gogineni, K. C. Jezek, and K. Kuivinen, Thickening of the western part of the Greenland ice sheet, *J. Glaciol.*, *44*, 653–658, 1998.

Thomas, R. H., C. H. Davis, E. Frederick, S. Manizade, W. Krabill, J. McConnell, and J. Sonntag, 20-year time series of Greenland ice-sheet thickness change from radar and laser altimetry, *Polar Geogr.*, *23*, 169–184, 1999.

Thomas, R., T. Akins, B. Csatho, M. Fahnestock, P. Gogineni, C. Kim, and J. Sonntag, Mass balance of the Greenland ice sheet at high elevations, *Science*, *289*, 426–428, 2000a.

Thomas, R., W. Abdalati, T. Akins, B. Csatho, E. Frederick, S. Gogineni, W. Krabill, S. Manizade, and E. Rignot, Substantial thinning of a major east Greenland outlet glacier, *Geophys. Res. Lett.*, *27*, 1291–1294, 2000b.

Thomas, R., B. Csatho, C. Davis, C. Kim, W. Krabill, S. Manizade, J. McConnell, and J. Sonntag, Mass balance of higher-elevation parts of the Greenland ice sheet, *J. Geophys. Res.*, this issue.

van der Veen, C. J., Interpretation of short-term ice-sheet elevation changes inferred from satellite altimetry, *Clim. Change*, *23*, 383–405, 1993.

van der Veen, C. J., and J. F. Bolzan, Interannual variability in net accumulation on the Greenland ice sheet: Observations and implications for mass balance measurements, *J. Geophys. Res.*, *104*, 2009–2014, 1999.

van de Wal, R. S. W., et al., Mass balance measurements in the Søndre Strømfjord area in the period 1990–1994, *Z. Gletscherkd. Glazialgeol.*, *31*, 57–63, 1995.

Wahr, J., T. van Dam, K. Larson, and O. Francis, Geodetic measurements in Greenland and their implications, *J. Geophys. Res.*, *106*, 16,567–16,581, 2001.

Wahr, J., T. van Dam, K. Larson, and O. Francis, GPS measurements of vertical crustal motion in Greenland, *J. Geophys. Res.*, this issue.

Weidick, A., Neoglacial change of ice cover and the related response of the earth's crust in West Greenland, *Rapp. Groenl. Geol. Unders.*, *159*, 121–126, 1993.

Winebrenner, D. P., R. J. Arthern, and C. A. Shuman, Mapping Greenland accumulation rates using observations of thermal emission at the 4.5-cm wavelength, *J. Geophys. Res.*, this issue.

Wingham, D. J., A. J. Ridout, R. Scharroo, R. Arthern, and C. K. Shum, Antarctic elevation change from 1992 to 1996, *Science*, *282*, 456–458, 1998.

Yoon, Y. T., Global orbit-error analysis using stochastic filtering methods, M. S. thesis, Univ. of Missouri, Columbia, 1998.

Zabel, I. H., K. C. Jezek, P. A. Baggeroer, and S. P. Gogineni, Radar observations of snow stratigraphy and melt processes on the Greenland ice sheet, *Ann. Glaciol.*, *21*, 40–44, 1995.

Zwally, H. J., and M. B. Giovinetto, Accumulation in Antarctica and Greenland derived from passive-microwave data: A comparison with contoured compilations, *Ann. Glaciol.*, *21*, 123–130, 1995.

Zwally, H. J., A. C. Brenner, J. A. Major, R. A. Bindschadler, and J. G. Marsh, Growth of Greenland ice sheet: Measurement, *Science*, *246*, 1587–1589, 1989.

Zwally, H. J., A. C. Brenner, J. P. DiMarzio, Technical Comment: Growth of the southern Greenland ice sheet, *Science*, *281*, 1251, 1998.

R. Thomas, EG&G, Inc., Bldg. N-159 Wallops Flight Facility, Wallops Island, VA 23337. (robert_thomas@hotmail.com)

(Received August 6, 2000; revised December 1, 2000;
accepted December 12, 2000.)